Heat and Mass transfer of MHD Casson nano fluid flow through a porous Media past a Vertical plate with Chemical, Hall and Dufour effects

D. Dastagiri Babu[1*], S. Venkateswarlu[1]

[1]Department of Mathematics, Rajeev Gandhi Memorial College of Engineering and Technology, Nandyal, Andhra Pradesh, India-518501

[*]Corresponding author: D. Dastagiri Babu

Abstract:

In this article, we analyses unsteady MHD free convection heat transfer flow of viscous incompressible, electrically conducting Casson nano fluid across an infinite vertical permeable plate using diffusion thermo, Hall current, magnetic field, chemical reaction, and thermo diffusion. Copper (Cu), Silver (Ag), Ferric Oxide (Fe_3O_4) based nanofluid has been considered. Partial differential equations are transformed into ordinary differential equations using non-dimensional variables and then solved using the three term simple perturbation technique. The profiles of velocity, temperature, and concentration are all numerically determined, as are the skin fiction coefficient, Nusselt number, and Sherwood number. The Casson, magnetic, hall, porosity, and Prandtl numbers are only a few of the regulating factors that are carefully explored in connection to the flow and heat transfer properties of the nanofluids Cu, Ag, and Fe_3O_4. It is evident that raising the Dufour number causes Mass and Heat transmission to increase. Hall parameter effects increase the velocity profile.

Key words: MHD, Casson nano fluid, Hall parameter, Dufour number, Perturbation method

 https://doi.org/10.5281/zenodo.14562181

1. Introduction

The fluids such as kerosene, engine oil and water have poor thermal conductivity. Hence they are not suitable to use in various processes such as production of chemicals, generation of power, oil refineries etc. In general, solid materials like Cu, Ag, Fe, and Al_2O_3 possess higher thermal conductivity when compared to liquids. By making use of this fact, Choi[1] invented nano fluids to overcome the problem of poor thermal conductivity of convectional fluids. He prepared nano fluids by suspending metallic/non-metallic particles in regular fluids and observed an enhancement in heat transfer ability of resultant nano fluid. Cu, Ag, and Fe_3O_4 are some materials which can be blended in regular fluids to prepare nano fluids. The suspension of these particles boosts the viscosity, thermal conductivity and thermal diffusivity of carrier fluids. Hence there are number of medical and engineering applications with nano fluids such as cooling of vehicle engines, nuclear systems cooling and cooling of microchips. Ganga et al.[2] discoursed the Over a vertical plate, a nano fluid with the Boungiorno model is subjected to MHD flow while internally producing or absorbing heat. The MHD nano fluids Cu, Al2O3 flow through a permeable vertical plate using convective heating were examined by Mutuku-Njane and Makinde[3]. Ahammad et al.[4] investigated radiation absorption with A semi-infinite vertical moving plate with a constant heating source exhibits, “Dufour effects on the rotational flow of a nanofluid Ag and TiO2. Vijaya and Reddy[5] have shown the magneto hydrodynamic casson fluid flow across a vertical porous plate in the presence of radiation, soret, and other chemical reaction effects.

Hazarika et al.[6] have investigated the effects of nanoparticles Cu, Ag, and Fe3O4 on the thermophoresis as well as viscous dissipation of MHD nanofluid over a stretched sheet in a porous regime. Dey et al.[7] investigated the MHD mixed convection reactive nano fluid flow on a vertical plate in the presence of slips assuming zero nanoparticle flux. A theoretical analysis of a Casson nanofluid across a vertical exponentially declining sheet with an inclined magnetic field was published by Ishtiaq and Nadeem[8]. Thamaraikannan et al.[9] have addressed the analytical analysis of magnetohydrodynamic non-Newtonian type Casson nano fluid flow over a porous channel with periodic body acceleration in their article. Babu et al.[10-11] investigated Heat and mass transfer on unsteady MHD flow of non-Newtonian fluid through a porous medium over an infinite vertical plate with hall effects. The authors[12–13] has focused on the MHD nano fluid flow across exponentially stretched sheets in a porous medium with convective boundary conditions

 https://doi.org/10.5281/zenodo.14562181

by applying response surface approaches. The authors[14–19] has developed the performance of the Casson nano fluid with varied nanoparticles over an endlessly permeable sliding plate in the presence of mass and warmth transfer.

The magnetic force terms absolute magnitude, direction, and current density is most strongly influenced by the Hall current. The convective flow problem with magnetic field under the effects of Hall currents is significant in light of applications in engineering in electric transformers, transmission lines, refrigeration coils, power generators, MHD accelerators, nanotechnology processing, nuclear energy systems using fluid metals, blood flow control, and heating elements. The research on Hall accelerators has the most applicability for the investigation of MHD flows with Hall current when the magnetic field is high and the gas density is low.

Many scientists have concentrated on studying non-Newtonian fluid flows because of the wide range of engineering and industrial uses. There are significant applications in the food engineering, petroleum production, plastics-related power engineering, polymer solutions, and melt industries. The Hall effect is substantial when the Hall parameter is big. The hall parameter is the difference between the frequency of atom-electron collisions and the frequency of electron cyclotrons. Rath et al.[20] have established the effects of viscous dissipation and dufour on MHD natural convective flow via an accelerating vertical plate with hall current. The effects of thermal diffusion and hall current on the radiative hydro magnetic flow of a spinning fluid in the presence of heat absorption were examined by Venkateswarlu et al.[21]. Sheri et al.[22] have investigated the effects of the hall current, dufour, and soret on transient MHD flow across an inclined porous plate using the finite element method. Suresh Kumar et al. have investigated the numerical research of the magneto hydrodynamic Casson micro fluid with activation energy, Hall current, and thermal radiation.

A strategy for approximating the solution to a problem by starting with the exact solution to a related, simpler problem is known as perturbation theory in applied mathematics. A crucial step in the process is the middle phase, which divides the problem into solvable and perturbative components. In perturbation theory, the solution is expressed as a power series in a minute parameter. The problem's accepted solution is mentioned in the first sentence. Higher power words in the series often become smaller as they go on. It is possible to create a rough "perturbation solution" by truncating the series, often maintaining just the first two terms.

 https://doi.org/10.5281/zenodo.14562181

However, in this case, we additionally take the third term into account to produce a better solution, the known problem's solution, and the first order perturbation adjustment.

A broad variety of fluids use perturbation theory, which reaches its most complex and cutting-edge applications in quantum field theory. The use of this technique in fluid mechanics is described by perturbation theory. In general, there is still a lot of research being done in this area across many academic areas. Abdelkhalek[24] has investigated the heat and mass transfer in MHD flow using perturbation approach. Paul and Talukdar[25] claim that the disruption of unsteady magneto hydrodynamic convective heat and material transport in a boundary layer slip flow through a vertical permeable plate is caused by thermal radiation and chemical reaction. The authors[26–27] examined the effects of a chemical reaction, heat transfer, and mass transfer over an MHD flow through a vertical porous wall using the perturbation technique.

The current study was motivated by the literature review mentioned above and focused on the MHD incompressible flow of mass and heat of a nano fluid through a vertical permeable sheet in a porous media under the influence of Hall, Chemical, and Dufour of nano fluids Copper (Cu), Silver (Ag), and Ferric oxide (Fe_3O_4). The boundary layer equations are resolved analytically, and the results are shown graphically. This work is unique in that it compares the effects of boundary layer free convection flow along a vertical sheet in water-based nanofluid on momentum, temperature, and concentration. This was inspired and motivated by the literatures cited as sources. Impacts of the nanoparticle volume fraction, magnetic body force and Dufour number contribute significantly to the uniqueness of the model under consideration.

2. Basic Equations

Let's think about the flow of a non-Newtonian nano fluid across a porous flat plate that is vertical. The flow is assumed that it flows in the direction that is taken across the plate and is normal to it in Figure 1, which depicts the physical contour of the issue. It is assumed that a B0 homogeneous external magnetic field is operating in the direction of. Because of the insignificant value of the Reynolds number, it is assumed that the induced magnetic field is irrelevant. The fluid and plate continue to be stationary at the same temperature and concentration. From a persistent source, thermal and concentration fluctuate harmonically over time near the surface. Additionally, the stream variables enable operations on z and t.

 https://doi.org/10.5281/zenodo.14562181

ISSN: 0369-8963

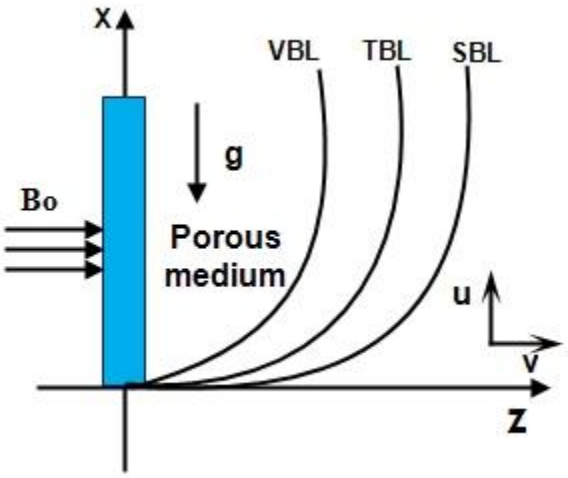

Fig. 1 Physical model of the problem

"The rheological equation of state for an isotropic and incompressible flow of Casson fluid (see References [28, 29]) is given by

$$\tau_{ij} = \begin{cases} 2\left[\mu_B + \dfrac{P_y}{\sqrt{2\pi}}\right] e_{ij}, \pi > \pi_c \\ 2\left[\mu_B + \dfrac{P_y}{\sqrt{2\pi}}\right] e_{ij}, \pi < \pi_c \end{cases} \tag{1}$$

Where π is the product based on the non-Newtonian fluid, p_y is the yield stress on the fluid, π_c is a critical value of this product, μ_B is the plastic dynamic viscosity of the non-Newtonian fluid $e_{i,j}$ is the $(i, j)^{th}$ component of deformation rate.

Under above boundary layer restrictions, the governing equations (see References [30, 31]) assumed as",

$$\frac{\partial v'}{\partial z'} = 0 \tag{2}$$

$$\left.\begin{aligned} \rho_{nf}\left[\frac{\partial u'}{\partial t'} + v'\frac{\partial u'}{\partial z'}\right] = \mu_{nf}\left(1+\frac{1}{\lambda}\right)\frac{\partial^2 u'}{\partial z'^2} - \frac{\mu_{nf}u'}{K'} - \frac{\sigma B_0{}^2}{\left(1+m^2\right)}u' + \left(\rho\beta\right)_{nf} g\left(T'-T'_\infty\right) \\ + \left(\rho\beta\right)_{nf} g\left(C'-C'_\infty\right) \end{aligned}\right\} \tag{3}$$

$$\left(\rho C_P\right)_{nf}\left(\frac{\partial T'}{\partial t'} + v'\frac{\partial T'}{\partial z'}\right) = \kappa_{nf}\frac{\partial^2 T'}{\partial z'^2} - Q'\left(T'-T'_\infty\right) + + \frac{D_m K_T}{C_s}\frac{\partial^2 C'}{\partial z'^2} \tag{4}$$

$$\frac{\partial C'}{\partial t'} + v'\frac{\partial C'}{\partial z'} = D_a\frac{\partial^2 C'}{\partial z'^2} - \kappa'(C'-C_\infty{}') \tag{5}$$

 https://doi.org/10.5281/zenodo.14562181

ISSN: 0369-8963

The boundary conditions are given by

$$\left.\begin{array}{l} u'(z',t')=0,\ \ T'=T_\infty{}',\quad C'=C'_\infty \quad for\ t'<0 \\ u'(z',t')=U_0, T'=T'_w+\left[T'_w-T'_\infty\right]\varepsilon e^{n't'} \\ C'=C'_w+\left[C'_w-C'_\infty\right]\varepsilon e^{n't'} \\ u'(z',t')=0,\ \ T'=T_\infty{}',\quad C'=C'_\infty \ \ as \qquad z'\to\infty \end{array}\right\} \begin{array}{l} \\ for\ t'\geq 0\ \ at\ \ z'=0 \\ \\ \\ \end{array} \tag{6}$$

Where u' and v' are velocity components of x and z direction respectively. Introduce the following nanofluid constants.

$$\rho_{nf}=(1-\phi)\rho_f+\phi\rho_s, (\rho\beta)_{nf}=(1-\phi)(\rho\beta)_f+\phi(\rho\beta)_s$$

$$(\rho C_p)_{nf}=(1-\phi)(\rho C_p)_f+\phi(\rho C_p)_s, \alpha_{nf}=\frac{K_{nf}}{(\rho C_p)_{nf}},$$

$$K_{nf}=K_f\left[\frac{K_s+2K_f-2\phi(K_f-K_s)}{K_s+2K_f+2\phi(K_f-K_s)}\right], \mu_{nf}=\frac{\mu_f}{(1-\phi)^{2.5}}$$

Where $v'=-V_0$ is constant which signifies normal in suction and injection case ($V_0>0$ and $V_0<0$) respectively.

Introducing the following non dimensional variables

$$\left\{\begin{array}{l} u=\dfrac{u'}{U_0},\ z^*=\dfrac{U_0 z'}{v_f},\ t=\dfrac{U^2{}_0 t'}{v_f},\ w=\dfrac{w'v_f}{U^2{}_0},\ \theta=\dfrac{T'-T'_\infty}{T'_w-T'_\infty},\ \psi=\dfrac{C'-C'_\infty}{C'_w-C'_\infty}, \\ Kr=\dfrac{K_1 v_f}{U_0{}^2},\ Pr=\dfrac{v_f}{\alpha_f},\ Gm=\dfrac{(\rho\beta^*)_{nf}\,g v_f(C'_w-C'_\infty)}{\rho_{nf}U_0{}^3},\ Gm=\dfrac{(\rho\beta)_{nf}\,g v_f(T'_w-T'_\infty)}{\rho_{nf}U_0{}^3}, \\ K=\dfrac{K'\rho_f U_0{}^2}{v_f{}^2},\ S_c=\dfrac{v_f}{D_m}, M=\dfrac{\sigma B_0{}^2 v_f}{\rho_{nf}U_0{}^2},\ \mathrm{Q}=\dfrac{Q'v_f{}^2}{K_f U_0{}^2},\ Du=\dfrac{D_m K_T}{C_s}\left(\dfrac{C'_w-C'_\infty}{T'_w-T'_\infty}\right) \end{array}\right\} \tag{7}$$

That governing Calculations (3)-(6) are abridged into their non-dimensional procedure by means of non-dimensional variables i.e. Equation (7) which is given by

$$A_1\left[\frac{\partial u}{\partial t}-\left(1+A\varepsilon e^{nt}\right)\frac{\partial u}{\partial z}\right]=\left(1+\frac{1}{\lambda}\right)A_4\frac{\partial^2 u}{\partial z^2}-\left[\frac{M^2}{\left(1+m^2\right)}+\frac{1}{K}\right]u+A_2G_r\theta+A_1G_c\psi \tag{8}$$

$$A_3\left[\frac{\partial\theta}{\partial t}-\left(1+\varepsilon e^{nt}\right)\frac{\partial\theta}{\partial z}\right]=\frac{1}{Pr}\left[A_5\frac{\partial^2\theta}{\partial z^2}-Q\theta\right]+\frac{Du}{Pr}\left(\frac{\partial^2\psi}{\partial y^2}\right) \tag{9}$$

$$\frac{\partial\psi}{\partial t}-\left(1+A\varepsilon e^{nt}\right)\frac{\partial\psi}{\partial z}=\frac{1}{Sc}\frac{\partial^2\psi}{\partial z^2}-Kc\psi \tag{10}$$

 https://doi.org/10.5281/zenodo.14562181

With boundary conditions

$$\begin{bmatrix} u=0,\ \theta=0,\ \psi=0 \quad for\ \ t<0 \\ u=1,\ \theta=1+\varepsilon e^{nt},\ \psi=1+\varepsilon e^{nt} \quad for\ \ t\geq 0 \quad at \quad z=0 \\ u=0,\ \theta=0,\ \psi=0 \quad for\ \ t\to\infty \end{bmatrix} \tag{11}$$

3. Solution of the Problem

Using the three phrase simple perturbation approach, the correlated non-linear PDE's Equations (8)–(10) with continuous boundaries (11) are solved (see References [32] and [34]). Below are the disturbed phrases:

$$u=u_0(z)+\varepsilon e^{nt}u_1(z)+\varepsilon^2 e^{2nt}u_2(z)+O(\varepsilon^3) \tag{12}$$

$$\theta=\theta_0(z)+\varepsilon e^{nt}\theta_1(z)+\varepsilon^2 e^{2nt}\theta_2(z)+O(\varepsilon^3) \tag{13}$$

$$\psi=\psi_0(z)+\varepsilon e^{nt}\psi_1(z)+\varepsilon^2 e^{2nt}\psi_2(z)+O(\varepsilon^3) \tag{14}$$

Equations (8) through (10) with Equations (12) through (14), where coefficient of a comparable power of ε and ε^2, in addition neglecting greater values of ε^3, we get subsequent calculations

Zero-order:

$$\left(1+\frac{1}{\lambda}\right)A_4\frac{d^2u_0}{dz^2}+A_1\frac{du_0}{dz}-\left(\frac{M^2}{(1+m^2)}+\frac{1}{K}\right)u_0=-A_2Gr\theta_0-A_2G_m\psi_0 \tag{15}$$

$$A_5\frac{d^2\theta_0}{dz^2}+A_3Pr\frac{d\theta_0}{dz}-Q\theta_0=-Du\psi_0'' \tag{16}$$

$$\frac{d^2\psi_0}{dz^2}+Sc\frac{d\psi_0}{dz}-Kc\,Sc\,\psi_0=0 \tag{17}$$

First-order:

$$\left(1+\frac{1}{\lambda}\right)A_4\frac{d^2u_1}{dz^2}+A_1\frac{du_1}{dz}-\left(\frac{M^2}{(1+m^2)}+\frac{1}{K}+nA_1\right)u_1=-A\frac{du_0}{dz}-A_2Gr\theta_1-A_2Gm\psi_1 \tag{18}$$

$$A_5\frac{d^2\theta_1}{dz^2}+A_3Pr\frac{d\theta_1}{dz}-\left(nA_3Pr+Q\right)\theta_1=-A_3Pr\frac{d\theta_0}{dz}-Du\psi_1'' \tag{19}$$

$$\frac{d^2\psi_1}{dz^2}+Sc\frac{d\psi_1}{dz}-Sc(Kc+n)\psi_1=-AScu\psi_0' \tag{20}$$

 https://doi.org/10.5281/zenodo.14562181

ISSN: 0369-8963

Second-order:

$$\left(1+\frac{1}{\lambda}\right)A_4\frac{d^2u_2}{dz^2}+A_1\frac{du_2}{dz}-\left(\frac{M^2}{\left(1+m^2\right)}+\frac{1}{K}+2nA_1\right)u_2=-A\frac{du_1}{dz}-A_2Gr\theta_2-A_2Gm\psi_2 \tag{21}$$

$$A_5\frac{d^2\theta_2}{dz^2}+A_3Pr\frac{d\theta_2}{dz}-\left(2nA_3Pr+Q\right)\theta_2=-A_3Pr\frac{d\theta_1}{dz}-Du\psi_2'' \tag{22}$$

$$\frac{d^2\psi_2}{dz^2}+Sc\frac{d\psi_2}{dz}-Sc(Kr+2n)\psi_2=-AScu\psi_1'' \tag{23}$$

The corresponding boundary conditions are

$$\left.\begin{array}{ll}\theta_0=1,\ \theta_1=1,\ \psi_0=1,\ \psi_1=1,\ u_0=1,\ u_1=0 & at\quad z=0\\ \theta_0=0,\ \theta_1=0,\ \psi_0=0,\ \psi_1=0,\ u_0=0,\ u_1=0 & at\quad z\to\infty\end{array}\right\} \tag{24}$$

Equations (15) through (23), when solved using boundary circumstances (24), provide the following results:

$$\begin{aligned}u(z,t)=&\left(c_5e^{-m_{14}z}+c_1e^{-m_2z}+c_4e^{-m_{14}z}\right)+\varepsilon\left(c_6e^{-m_{14}z}+c_9e^{-m_{10}z}+c_{15}e^{-m_8z}+c_{16}e^{-m_4z}+c_{17}e^{-m_2z}\right)\mathrm{e}^{nt}\\&+\varepsilon^2\left(\begin{array}{c}c_{38}e^{-m_{18}z}+c_{19}e^{-m_{14}z}+c_{24}e^{-m_{12}z}+c_{33}e^{-m_{10}z}+c_{34}e^{-m_8z}\\+c_{35}e^{-m_2z}+c_{36}e^{-m_4z}+c_{37}e^{-m_5z}\end{array}\right)\mathrm{e}^{2nt}\end{aligned} \tag{25}$$

$$\begin{aligned}\theta(z,t)=&\left(b_2e^{-m_8z}+b_1e^{-m_8z}\right)+\varepsilon\left(b_8e^{-m_{10}z}+b_3e^{-m_8z}+b_5e^{-m_4z}+b_7e^{-m_2z}\right)\mathrm{e}^{nt}\\&+\varepsilon^2\left(b_{18}e^{-m_{12}z}+b_9e^{-m10z}+b_{10}e^{-m_8z}+b_{13}e^{-m_5z}+b_{16}e^{-m_4z}+b_{17}e^{-m_2z}\right)\mathrm{e}^{2nt}\end{aligned} \tag{26}$$

$$\psi(z,t)=(e^{-m_2z})+\varepsilon(a_2e^{-m_4z}+a_1e^{-m_2z})\,\mathrm{e}^{nt}+\varepsilon^2\left(a_5e^{-m_5z}+a_3e^{-m_4z}+a_4e^{-m_2z}\right)\mathrm{e}^{2nt} \tag{27}$$

The shear stress on the platter is specified as

$$\begin{aligned}\tau=\left(\frac{\partial u}{\partial t}\right)_{z=0}=&\left(-m_{14}c_5-m_8c_1-m_2c_4\right)+\varepsilon\left(-m_{14}c_6-m_{10}c_9-m_8c_{15}-m_4c_{16}-m_2c_{17}\right)e^{nt}\\&+\varepsilon^2\left(-m_{18}c_{38}-m_{14}c_{19}-m_{12}c_{24}-m_{10}c_{33}-m_8C_{34}-m_2c_{35}-m_4C_{36}-m_5c_{37}\right)e^{2nt}\end{aligned} \tag{28}$$

The rate of heat transfer is assumed by way of

$$\begin{aligned}Nu=-\left(\frac{\partial\theta}{\partial t}\right)_{z=0}=&\left(-m_8b_2-m_2b_1\right)+\varepsilon\left(-m_{10}b_8-m_8b_3-m_4b_5-m_2b_7\right)e^{nt}\\&+\varepsilon^2\left(-m_{12}b_{18}-m_{10}b_9-m_8b_{10}-m_5b_{13}-m_4b_{16}-m_2b_{17}\right)e^{2nt}\end{aligned} \tag{29}$$

The rate of mass transfer is agreed by way of

$$Sh=-\left(\frac{\partial\psi}{\partial t}\right)_{z=0}=\left(-m_2\right)+\varepsilon\left(-m_4a_2-m_2a_1\right)e^{nt}+\varepsilon^2\left(-m_5a_5-m_4a_3-m_2a_4\right)e^{2nt} \tag{30}$$

 https://doi.org/10.5281/zenodo.14562181

4. Results and Discussion

Here, we present and talk about the outcomes that were computed using the three term simple peturbation technique analytically. Additionally, an illutrated in Figures 2-10 and Tables 2 and 3, the perfomance of Casson nano fluid flow velocity profiles (u), temperature profiles (θ) under the impact of fluid parameters, that is Dufour parameter (Du), Prandtl parameter (Pr), Hall parameter (m) ,Casson parameter (λ), magnetic parameter (M), and nano particle volume fraction (ϕ) is explored. For these purposes, numerical solutions are carried out, with $s=1, \phi=0.10,\ Sc=0.22, Pr=0.72, Kr=0.5, M=1, Du=1, Gr=2, Gm=2;$ The results are presented for three kinds of nano fluids viz. Cu, Ag, Fe_3O_4. The thermophysical properies of nanofluids are showed into Table 1.

TABLE 1 Thermo physical proprties (see Reference [33]):

Physical Properties	$\rho(kgm^{-3})$	$\beta\times10^{-5}(k^{-1})$	$k(wm^{-1}\ k^{-1})$	$C_p(Jk^{-1}g^{-1}\ k^{-1})$
H_2O	997.3	21	0.613	4179
Cu	8933	1.67	401	385
Ag	10500	1.89	429	240
Fe_3O_4	5180	0.7	9.7	670

Magnetic field's impact on the velocity profile of the Cu, Ag, Fe_3O_4 nano fluids is portrayed in the Figure 2. The fluid flow is opposed by the Lorentz force, which is produced by the existence of a magnetic field. This forces amplitude is directly proportional to the magnitude of (M). Therefore, the Lorentz forces is strengthened as (M) increases. Thus, the momentum is observed to diminishes with higher values of (M). This, in turn, increases the fluid flow resistance.

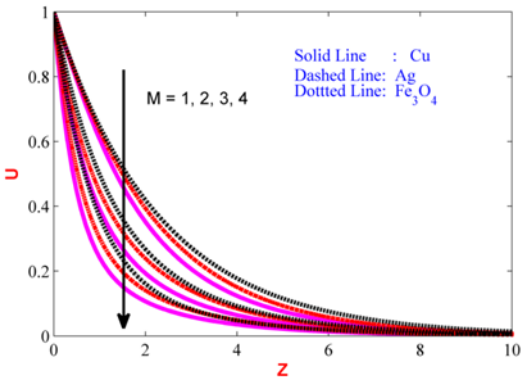

Fig. 2 Influence of M on u

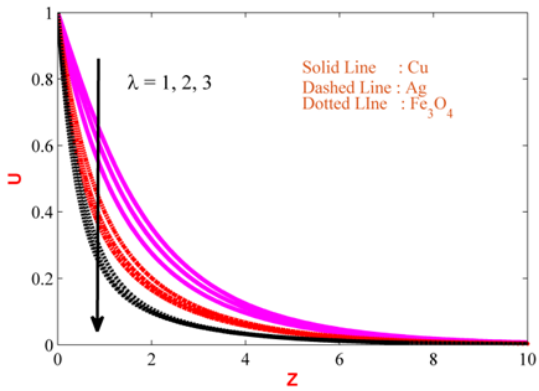

Fig. 3 Influence of λ on u

Figure 3 shows the impact of Casson fluid parameter (λ) for various nano fluids such as Cu, Ag,

https://doi.org/10.5281/zenodo.14562181

and Fe_3O_4 on the distribution of velocity profile. The velocity profiles are likewise raised while the Casson fluid parameter is increased. It has been observed that raising the prompt values causes the plastic dynamic constancy to expand, which creates resistance to fluid flow. The thickness of the thermal boundary layer and momentum both decrease as a result.

The velocity profile (U) plus the related boundary layer width are rising functions of the Hall parameter (m), as can be seen in Figure 4. This is as a result of the drag force $-\left[\frac{M^2}{\left(1+m^2\right)}+\frac{1}{K}\right]u$ in Equation (8) is diminished with an increase in the Hall parameter (m) which in turn enhances the velocity profile.

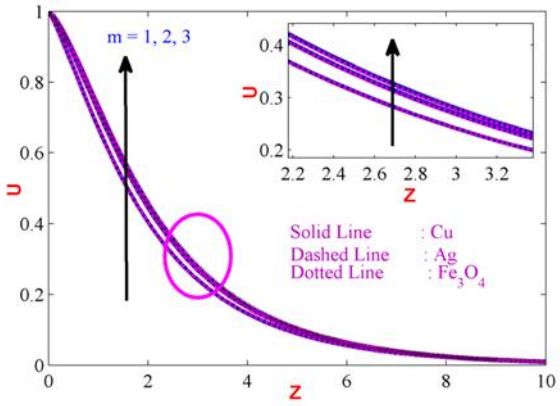

Fig. 4 Influence of (m) on u

Figure (5) and Figure (6) portray the variations of Velocity (U) and Temperature profiles of nano fluid towards the nanoparticle volume fraction (ϕ) for nanoparticles of Cu, Ag, and Fe_3O_4 at $Sc = 0.22, Pr = 0.72, Gr = Gm = 2, Kr = 0.5$. When (ϕ) increases, the thermal conductivity of the fluid increases as a result the thermal boundary layer increases and therefore, (θ) profiles of the nanofluid escalated, Velocity (U) profiles shows an opposite behaviour for (ϕ) as compared with the Figure (6) for various nano particles.

The relationship between the Prandtl number and the velocity of Cu, Ag, and Fe_3O_4 nanoparticles having a given volume fraction is shown in Figures (7A)–(7C). Because of the viscosity-induced resistance to fluid flow, greater Prandtl numbers show decrease in the velocity boundary layer. The flow rate is improved by the plate's enhanced external cooling. Figures (7D)–(7F) show the effect of Pr on the temperature profile of Cu, Ag, and Fe_3O_4 nanoparticles

https://doi.org/10.5281/zenodo.14562181

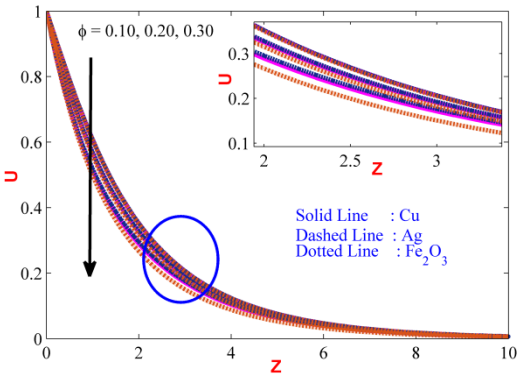

Fig. 5 Influence of ϕ on u

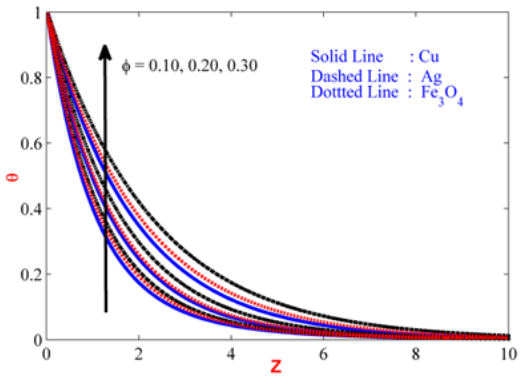

Fig. 6 Influence of ϕ on θ

with a given volume percent. Figures (7D)–(7F) show that when the values of Pr increase, the temperature field decreases. The reduction in thermal conducting properties is the major cause of the temperature profile's decline. However, the increased temperature field in the flow is also a result of dissipation effects. Additionally, with increasing values of Pr, the thickness of the temperature boundary layer diminishes. This drop in temperature is primarily caused by the magnified Pr values, which significantly reduce thermal diffusivity and, as a result, reduce the thickness of the temperature boundary layer. Pr often refers to very viscous substances like oils and other liquids. This finding leads to the conclusion that Pr has a negative relationship with the temperature field.

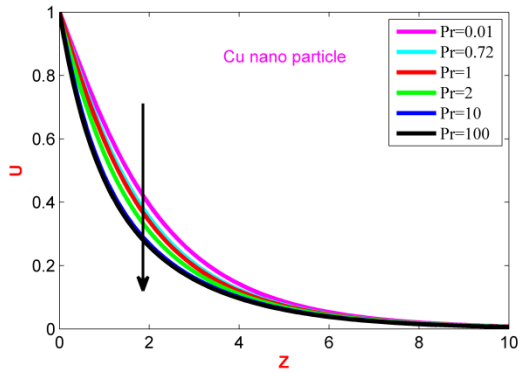

Fig. 7A Influence of *Pr* on *u* for *Cu* nano particle

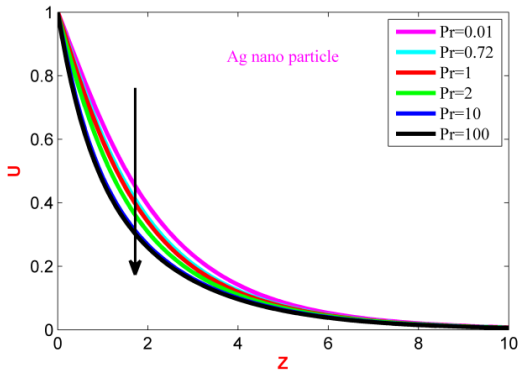

Fig. 7B Influence of *Pr* on *u* for *Ag* nano particle

https://doi.org/10.5281/zenodo.14562181

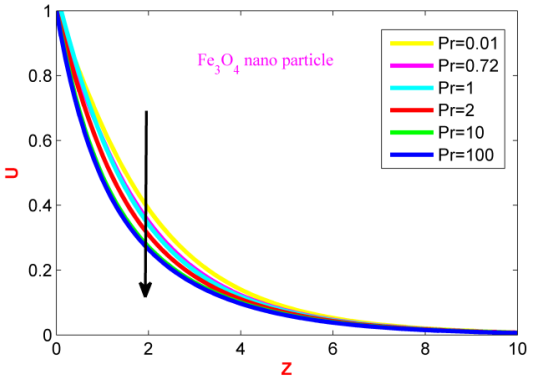

Fig. 7C Influence of Pr on u for Fe_3O_4 nano particle

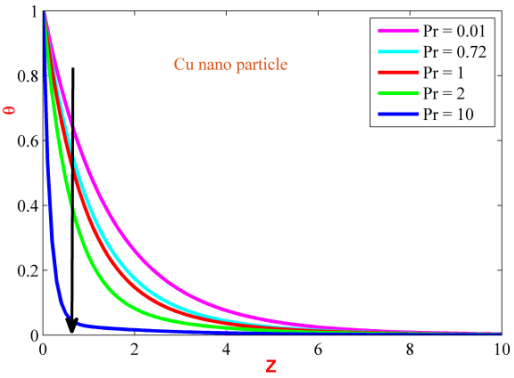

Fig. 7D Influence of Pr on θ for Cu nano particle

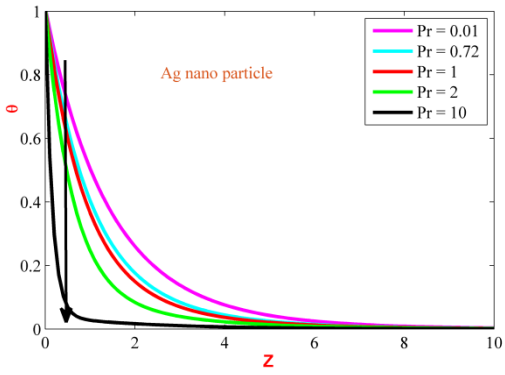

Fig. 7E Influence of Pr on θ for Ag nano particle

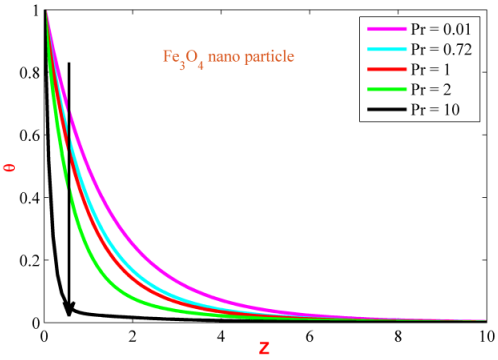

Fig. 7F Influence of Pr on θ for Fe_3O_4 nano particle

For nanoparticles of Cu, Ag, and Fe3O4, Figure (8A)–(8D) illustrates the Dufour impact on speed and temperature profile distributions. For the nano fluids, it is observed that the boundary layer thickness increases with Du. As the Dufour number increases, the hydrodynamic boundary layer's thickness increases, as seen in Figures (8A)–(8C). The effects of Du on the temperature gradients inside the boundary layer are shown in Figure (9). The temperature of the nanofluid for the nanoparticles Cu, Ag, and Fe3O4 is seen to be increasing with the increasing values of Du. Specifically, Du makes the thermal barrier layer thicker. Physically, reducing Du distinctly lessens the impact of taxonomic gradients upon the temperature field, resulting in distinctly lower temperature function values and a cooling of the boundary layer regime. Figure (10) shows the effects of a specific reaction parameter on concentration profile with fixed values for $s = 0.1, Sc = 0.22, Pr = 0.72, n = 0.1$. In general, it is shown that the decreasing concentration field is often seen for damaging chemical reactions. As a result, Figure (10) clearly shows that the concentration distribution declines throughout a destructive chemical reaction.

https://doi.org/10.5281/zenodo.14562181

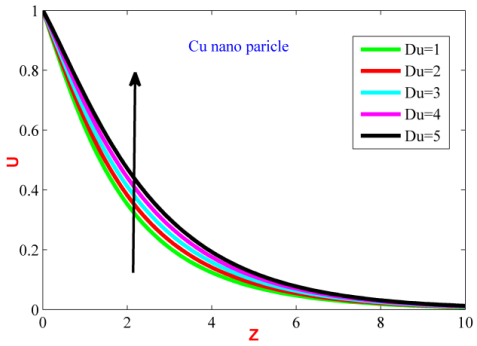

Fig. 8A Influence of *Du* on *u* for *Cu* nano particle

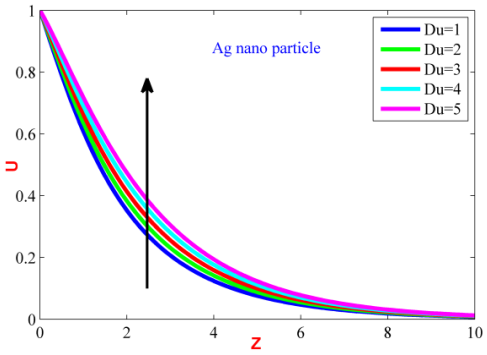

Fig. 8B Influence of *Du* on *u* for *Ag* nano particle

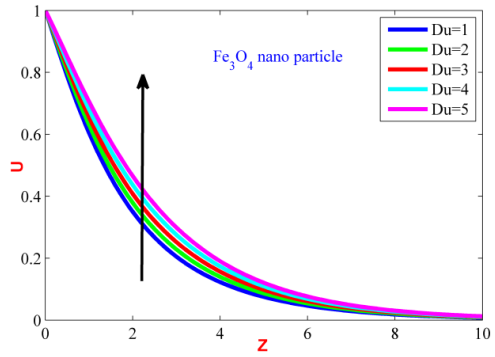

Fig. 8C Influence of *Du* on *u* for Fe_3O_4 nano particle

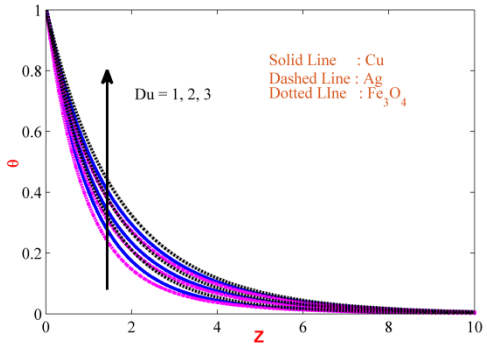

Fig. 9 Influence of *Du* on θ

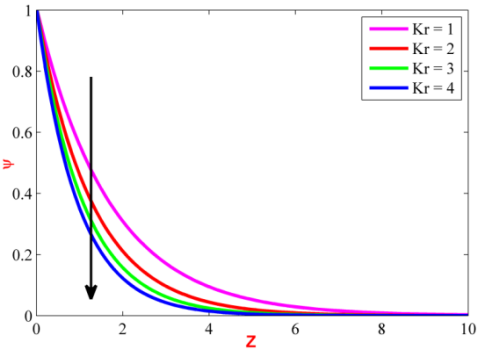

Fig. 10 Influence of *Kr* on ψ

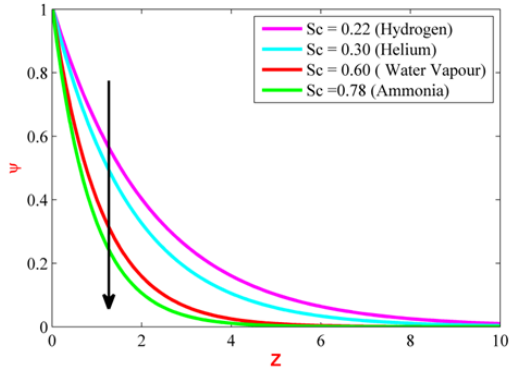

Fig. 11 Influence of *Sc* on ψ

Figure (11), which shows the effect of the Schmidt number on a concentration profile with constant values, describes this effect. The concentration field in the flow zone diminishes as the Schmidt number rises, as shown by Figure (11). These arguments support this fact: A little increase in the Schmidt number causes the mass diffusion coefficient to be reduced, which lowers the concentration field in the flow zone. The concentration field is also shown to be a

https://doi.org/10.5281/zenodo.14562181

decreasing function of Sc. Additionally, when Sc values increase, the thickness of the concentration boundary layer diminishes which is seen in Figure (11)

The numerical values of the Skin-friction coefficient and Nusselt number for the nano particles Cu, Ag, Fe_3O_4 are presented in Tables 2 and 3. From Table 2, it is observed that the Skin-friction coefficient escalates with enhancing the values of Dufour number (Du) and Casson fluid parameter (λ), While it diminishes with rising the values of Magnetic field parameter (M), nano particle volume fraction (ϕ), Chemical reaction parameter (Kr), Prandtl number (Pr), Schmidt number (Sc) for the nano particles Cu, Ag, Fe_3O_4. From Table 3, it is clear that the local Nusselt number escalates with raising the values of nano particle volume fraction (ϕ), Chemical reaction parameter (Kr), and Schmidt number (Sc),While it diminishes with raising the values of Dufour number (Du) and Prandtl number (Pr) for the nano fluids Cu, Ag, Fe_3O_4.

TABLE 2: Skin-friction for various parameters

M	ϕ	Du	λ	Kr	Pr	Sc	τ		
							Cu	Ag	Fe_3O_4
1	0.1	1	1	0.5	0.72	0.22	-0.2720	-0.2787	-0.2869
2							-0.6979	-0.7095	-0.6960
3							-1.1918	-1.2080	-1.1748
4							-1.6906	-1.7101	-1.6623
	0.15						-0.3085	-0.3183	-0.3310
	0.20						-0.3340	-0.3458	-0.3644
	0.25						-0.3473	-0.3597	-0.3868
		2					-0.2238	-0.2286	-0.2437
		3					-0.1756	-0.1784	-0.2004
		4					-0.1273	-0.1282	-0.1571
			2				-0.2716	-0.2809	-0.2896
			3				-0.2702	-0.2807	-0.2894
			4				-0.2690	-0.2803	-0.2892
				1.0			-0.3227	-0.3320	-0.3305
				1.5			-0.3540	-0.3648	-0.3578
				2.0			-0.3759	-0.3879	-0.3776
					1		-0.3026	-0.3082	-0.3099
					2		-0.4038	-0.3742	-0.3874
					3		-0.4443	-0.4551	-0.4438
						0.30	-0.3136	-0.3224	-0.3226
						0.60	-0.4004	-0.4142	-0.4042
						0.78	-0.5629	-0.5540	-0.4533

 https://doi.org/10.5281/zenodo.14562181

TABLE 3: Nusselt number for various parameters

ϕ	Du	Kr	Pr	Sc	Nu		
					Cu	Ag	Fe_3O_4
0.1	1	0.5	0.72	0.22	-0.9710	-0.9644	-1.0050
0.15					-0.8506	-0.8428	-0.8978
0.20					-0.7414	-0.7332	-0.8006
0.25					-0.6399	-0.6320	-0.7111
	2				-0.8371	-0.8310	-0.8643
	3				-0.7032	-0.6976	-0.7236
	4				-0.5693	-0.5642	-0.5829
		1.0			-0.9078	-0.9014	-0.9383
		1.5			-0.8549	-0.8486	-0.8822
		2.0			-0.8081	-0.8018	-0.8326
			1		-1.0882	-1.0784	-1.1274
			2		-1.5702	-1.5467	-1.6309
			3		-2.1218	-2.0829	-2.2070
				0.30	-0.9204	-0.9140	-0.9517
				0.60	-0.7274	-0.7213	-0.7473
				0.78	-0.6099	-0.6040	-1.0157

CONCLUSIONS:

Analytical solutions are provided for the MHD boundary layer flow of different nanofluids across a vertical sheet for the Casson model according to the boundary conditions. Additionally, impacts for the profiles, several values of the already-existing parameters are investigated of velocity, temperature, and concentration. The key findings of the current analysis are presented below.

- The thickness of the momentum boundary layer decreases as the magnetic parameter M increases.
- The distribution of the velocity profile improves as the hall parameter, m, rises.
- The nano fluids' velocity field is suppressed as the Casson parameter raises.
- When the volume percentage of nanoparticles rises, contradictory behaviors are shown in terms of momentum and thermal boundary layer thickness.
- As Prandtl number Pr increases, the momentum as well as thermal boundary layer thickness increase.
- As the Dufour number rises, the distributions of velocity and temperature are improved.

 https://doi.org/10.5281/zenodo.14562181

ISSN: 0369-8963

- The Fe_3O_4-water nanofluid always has a greater nevertheless; the temperature profiles show the reverse trend. velocity, followed by the Cu and Ag water nanofluids.
- The Casson fluid parameter increases and decreases as in the M, Kr, Pr, Sc, and the skin friction coefficient increases and lowers with an augmenting in the Dufour number (Du).
- The Nusselt number increases together with increases in the Du, Kr, Sc, and, while it lowers along with increases in the Pr.

NOMENCLATURE

u, v velocity field components in x, z direction
Du Dufour number
Gr thermal Grashof number
Gm mass Grashof number
g acceleration due to gravity (m/s^2)
m Hall Parameter
λ Casson Parameter
M Magnetic parameter
Pr Prandtl number
Q Heat absorption parameter (J/K)
Sc Schmidt number
Sh Sherwood number
Nu Nusselt number
Kr Chemical reaction number (W/mk)
u Velocity profile
θ temperature profile

Greek Symbols:

α_f thermal diffusivity of base fluid, m^2/s
α_{nf} thermal diffusivity of nano fluid, m^2/s
κ_f thermal conductivity of base fluid, W/(mk)
κ_{nf} thermal conductivity of base fluid
μ_f Dynamic viscosity of base fluid ($kgm^{-1}s^{-1}$)
μ_{nf} Dynamic viscosity of nano fluid ($kgm^{-1}s^{-1}$)
ρ_f Density of base fluid (kg/m^3)
ρ_{nf} Density of nano fluid (kg/m^3)
$(\rho\beta)_f$ thermal expansion coefficient of base fluid (kg/Km^3)
$(\rho\beta)_{nf}$ thermal expansion coefficient of nano fluid (kg/Km^3)
$(\rho\beta)_s$ thermal expansion coefficient of nano particles (kg/Km^3)
$(\rho C_p)_s$ heat capacitance of the nano particles
$(\rho C_p)_f$ heat capacitance of the base fluid
$(\rho C_p)_n$ heat capacitance of the nano fluid
ψ Concentration profile

Subscripts

f Fluid
s Nano particle
nf Nano fluid

https://doi.org/10.5281/zenodo.14562181

REFERENCES

1. Choi. SUS. Enhancing thermal conductivity of fluids with nanoparticles, Developments and applications of non-Newtonian flows, ASME FED 231/MD 66 (1995), 99–105.
2. Ganga B, Ansari SM, Ganesh NV, Hakeem AA. MHD flow of Boungiorno model nanofluid over a vertical plate with internal heat generation/absorption. Propuls Power Res. 2016;5(3):211-22. https://doi.org/10.1016/j.jppr.2016.07.003
3. Mutuku-Njane WN, Makinde OD. MHD nanofluid flow over a permeable vertical plate with convective heating. J Comput Theor Nanosci. 2014;11(3):667-75. DOI: 10.1166/jctn.2014.3410
4. Ameer Ahamad N, Veera Krishna M, Chamkha AJ. Radiation-absorption and Dufour effects on magneto hydrodynamic rotating flow of a nanofluid over a semi-infinite vertical moving plate with a constant heat source. J Nanofluids. 2020;9(3):177-86. DOI: https://doi.org/10.1166/jon.2020.1743
5. Vijaya K, Reddy GV. Magneto hydrodynamic casson fluid flow over a vertical porous plate in the presence of radiation, soret and chemical reaction effects. J Nanofluids. 2019;8(6):1240-8. DOI: 10.1166/jon.2019.1684
6. Hazarika S, Ahmed S, Chamkha AJ. Investigation of nanoparticles Cu, Ag and Fe3O4 on thermophoresis and viscous dissipation of MHD nanofluid over a stretching sheet in a porous regime: a numerical modeling. Math Comput Simul. 2021;182:819-37. DOI: 10.1016/j.matcom.2020.12.005
7. Dey S, Ghosh S, Mukhopadhyay S. MHD mixed convection chemically reactive nanofluid flow over a vertical plate in presence of slips and zero nanoparticle flux. Waves Random Complex Media. 2023:1-20. https://doi.org/10.1080/17455030.2022.2148014
8. Ishtiaq B, Nadeem S. Theoretical analysis of Casson nanofluid over a vertical exponentially shrinking sheet with inclined magnetic field. Waves Random Complex Media. 2022;23:1-7. https://doi.org/10.1080/17455030.2022.2103206
9. Thamaraikannan N, Karthikeyan S, Chaudhary DK, Kayikci S. Analytical investigation of magnetohydrodynamic non-Newtonian type Casson nanofluid flow past a porous channel with periodic body acceleration. Complexity. 202117;2021:1-7. https://doi.org/10.1155/2021/7792422

10. Babu, D. D., Venkateswarlu, S., & Reddy, E. K. (2018). Heat and mass transfer on MHD flow of Non-Newtonian fluid over an infinite vertical porous plate with Hall effects. Int. J. Pure and Appl. Math., 119(15), 87-103. https://acadpubl.eu/hub/2018-119-15/4/633.pdf
11. Babu, D. D., Venkateswarlu, S., & Reddy, E. K. (2017, July). Heat and mass transfer on unsteady MHD free convection rotating flow through a porous medium over an infinite vertical plate with hall effects. In *AIP Conference Proceedings* (Vol. 1859, No. 1). AIP Publishing.
12. Hussain S, Rasheed K, Ali A, Vrinceanu N, Alshehri A, Shah Z. A sensitivity analysis of MHD nanofluid flow across an exponentially stretched surface with non-uniform heat flux by response surface methodology. Sci Rep. 2002;12(1):18523. https://doi.org/10.1038/s41598-022-22970-y.
13. Hayat, T., M. Imtiaza, A. Alsaedib and R. Mansoora (2014). MHD flow of nanofluids over an exponentially stretching sheet in a porous medium with convective boundary conditions. Chin Phys B; 23(5), 054701. DOI: 10.1088/1674-1056/23/5/054701
14. Ravindranath Reddy G, Ramakrishna Reddy K. Casson nanofluid performance on MHD convective flow past a semi-infinite inclined permeable moving plate in presence of heat and mass transfer. Heat Transf. 2022;51(8):7307-27. https://doi.org/10.1002/htj.22645
15. Biswal MM, Swain K, Dash GC, Mishra S. Study of chemically reactive and thermally radiative Casson nanofluid flow past a stretching sheet with a heat source. Heat Transf. 2023;52(1):333-53. https://doi.org/10.1002/htj.22697.
16. Ali B, Shafiq A, Manan A, Wakif A, Hussain S. Bioconvection: Significance of mixed convection and mhd on dynamics of Casson nanofluid in the stagnation point of rotating sphere via finite element simulation. Math and Comput Simul. 2022;194:254-68. https://doi.org/10.1016/j.matcom.2021.11.019
17. Li YX, Rehman MI, Huang WH, Khan MI, Khan SU, Chinram R, Kadry S. Dynamics of Casson nanoparticles with non-uniform heat source/sink: A numerical analysis. Ain Shams Eng. 2022;13(1);101496. https://doi.org/10.1016/j.asej.2021.05.010
18. Biswal MM, Swain K, Dash GC, Mishra S. Study of chemically reactive and thermally radiative Casson nanofluid flow past a stretching sheet with a heat source. Heat Transf. 2023;52(1):333-53. https://doi.org/10.1002/htj.22697

19. Haq RU, Nadeem S, Khan ZH, Okedayo TG. Convective heat transfer and MHD effects on Casson nanofluid flow over a shrinking sheet. Centr eur j phys. 2014;12:862–871. https://doi.org/10.2478/s11534-014-0522-3
20. Rath C, Nayak A, Panda S. Impact of viscous dissipation and Dufour on MHD natural convective flow past an accelerated vertical plate with Hall current. Heat Transf. 2022;51(6):5971-95. https://doi.org/10.1002/htj.22577
21. Venkateswarlu M, Makinde OD, Reddy PR. Influence of Hall current and thermal diffusion on radiative hydromagnetic flow of a rotating fluid in presence of heat absorption. J Nanofluids. 2019;8(4):756-66. DOI: 10.1166/jon.2019.1638
22. Sheri SR, Megaraju P, Rajashekar MN. Impact of Hall Current, Dufour and Soret on transient MHD flow past an inclined porous plate: Finite element method. Mater Today: Proc. 2022;59:1009-21. https://doi.org/10.1016/j.matpr.2022.02.279
23. Suresh Kumar Y, Hussain S, Raghunath K, Ali F, Guedri K, Eldin SM, Khan MI. Numerical analysis of magnetohydrodynamics Casson nanofluid flow with activation energy, Hall current and thermal radiation. Sci Rep. 2023;13(1):4021. https://doi.org/10.1038/s41598-023-28379-5
24. Abdelkhalek MM. Heat and mass transfer in MHD flow by perturbation technique. Comp Mater Sci. 2008;43(2):384-91. https://doi.org/10.1016/j.commatsci.2007.12.003
25. Pal D, Talukdar. B. Perturbation analysis of unsteady magneto hydrodynamic convective heat and mass transfer in a boundary layer slip flow past a vertical permeable plate with thermal radiation and chemical reaction. Commun Nonlinear Sci Numer Simul. 2010;15: 1813–1830. DOI: 10.1016/j.cnsns.2009.07.011
26. Gireesha BJ, Mahanthesh B. Perturbation solution for radiating viscoelastic fluid flow and heat transfer with convective boundary condition in non-uniform channel with hall current and chemical reaction. Int Sch Res Not. 2013;81:9354. https://doi.org/10.1155/2013/935481
27. Ahmed S, Zueco J, López-González LM. Effects of chemical reaction, heat and mass transfer and viscous dissipation over a MHD flow in a vertical porous wall using perturbation method. Int J of Heat and Mass Transf. 2017;104:409-18. https://doi.org/10.1016/j.ijheatmasstransfer.2016.07.076

28. Reddy JV, Sugunamma V, Sandeep N. Slip flow of MHD casson-nanofluid past a variable thickness sheet with joule heating and viscous dissipation: A comparative study using three base fluids. J Nanofluids. 2018;7(6):1113-21. DOI: 10.1166/jon.2018.1540
29. Venkateswarlu S, Babu DD, Reddy EK. Approximation Of Casson fluid In Conducting Field Past A Plate In The Presence Of Dufour, Radiation And Chemical Reaction Effects. J Mech Con Math Sci. 2020;15(5):1-19. DOI: 10.26782/jmcms.2020.05.00001
30. Kune R, Naik HS, Reddy BS, Chesneau C. Role of Nanoparticles and Heat Source/Sink on MHD Flow of Cu-H2O Nanofluid Flow Past a Vertical Plate with Soret and Dufour Effects. Math Comput Appl. 2022 28;27(6):102. https://doi.org/10.3390/mca27060102
31. Oahimire JI, Olajuwon BI, Effect of Hall current and thermal radiation on heat and mass transfer of a chemically reacting MHD flow of a micropolar fluid through a porous medium. Journal of King Saud University-Engineering Sciences. 2014;26(2):112-121. https://doi.org/10.1016/j.jksues.2013.06.008
32. Babu DD, Venkateswarlu S, Keshava Reddy E. Multivariate Jeffrey fluid flow past a vertical plate through porous medium. J Appl Comput Mech. 2020;6(3):605-16. DOI: 10.22055/JACM.2019.28988.1534
33. Abbasi FM, Maimoona Gul, Shehzad. Effectiveness of temperature-dependent properties of Au, Ag, Fe_3O_4, Cu nanoparticles in peristalsis of nanofluids. Int. Commun. in Heat Mass transf. DOI: 10.1016/j.icheatmasstransfer.2020.104651